Quaternary International 470 (2018) 26–37

Contents lists available at ScienceDirect

Quaternary International

journal homepage: www.elsevier.com/locate/quaint

Palaeoclimate, glacier and treeline reconstruction based on geomorphic evidences in the Mongun-Taiga massif (south-eastern Russian Altai) during the Late Pleistocene and Holocene

Dmitry Ganyushkin [a,*], Kirill Chistyakov [a], Ilya Volkov [a], Dmitry Bantcev [a], Elena Kunaeva [b], Dagmar Brandová [c], Gerald Raab [c], Marcus Christl [d], Markus Egli [c]

[a] Saint-Petersburg State University, Department of Physical Geography and Landscape Planning, Saint-Petersburg 199178, 10 liniya V.O., h.33-35, Russian Federation
[b] Pushkin Leningrad State University, 10 Peterburgskoe shosse, St Petersburg (Pushkin) 196605, Russian Federation
[c] Department of Geography, University of Zurich, Winterthurerstrasse 190, CH-8057 Zurich, Switzerland
[d] Laboratory of Ion Beam Physics, ETH Zurich, 8093 Zurich, Switzerland

ARTICLE INFO

Article history:
Received 30 March 2017
Received in revised form
27 November 2017
Accepted 17 December 2017
Available online 26 December 2017

Keywords:
Palaeoclimate reconstruction
Pleistocene
Holocene
Arid mountains of Altai
Treeline
Glaciers

ABSTRACT

Little is known about the extent of glaciers and dynamics of the landscape in south-eastern Russian Altai. The effects of climate-induced fluctuations of the glaciers and the upper treeline of the Mongun-Taiga mountain massif were, therefore, reconstructed on the basis of in-situ, multiannual observations, geomorphic mapping, radiocarbon and surface exposure dating, relative dating (such as Schmidt-hammer and weathering rind) techniques and palaeoclimate-modelling.

During the maximal advance of the glaciers, their area was 26-times larger than now and the equilibrium line of altitude (ELA) was about 800 m lower. Assuming that the maximum glacier extent took place during MIS 4, then the average summer temperatures were 2.7 °C cooler than today and the amount of precipitation 2.1 times higher. Buried wood trunks by a glacier gave ages between 60 and 28 cal ka BP and were found 600–700 m higher than the present upper treeline. This evidences a distinctly elevated treeline during MIS 3a and c. With a correction for tectonics we reconstructed the summer warming to have been between 2.1 and 3.0 °C. During MIS 3c, the glaciated area was reduced to less than 0.5 km^2 with an increase of the ELA of 310–470 m higher than today. Due to higher precipitation, the glaciated area during MIS 3a was close to the current ELA. Exposure dating (^{10}Be) would indicate that the maximum glacier extension was 24 ka BP, but the results are questionable. From a geomorphic point of view, the maximum extent can more likely be ascribed to the MIS4 stage. We estimate a cooling of summer temperature of − 3.8 to − 4.2 °C and a decrease in precipitation of 37–46% compared to the present-day situation. Samples of wood having an age of 10.6–6.2 cal ka BP were found about 350 m higher than the present treeline. It seems that the summer temperature was 2.0–2.5 °C higher and annual precipitation was double that of the present-day. For that period, the reconstructed glaciation area was 1 km^2 less than today. Three neoglacial glacier advances were detected. The glaciers covered about double the area during the Little Ice Age (LIA), summer cooling was 1.3 °C with 70% of the present-day precipitation. The reconstructed amplitude of climatic changes and the shift of the altitudinal zones show that the landscape has reacted sensitively to environmental changes and that dramatic changes may occur in the near future.

1. Introduction

The Altai mountain region is situated at the border of Central Asia and Siberia and is an area having numerous geomorphic features that clearly display the variability of climatic conditions and landscape dynamics. The Altai mountains span four different

* Corresponding author. Petersburg State University, Institute of Earth Sciences, Department of Physical Geography and Landscape Planning, Saint-Petersburg 199178, 10 liniya V.O., h.33-35, Russian Federation.
E-mail address: d.ganyushkin@spbu.ru (D. Ganyushkin).

https://doi.org/10.1016/j.quaint.2017.12.031
1040-6182/

countries (Russia, Mongolia, Kazakhstan and China). Due to the remoteness of the Altai mountains, this region is still very poorly studied in regard to the Holocene and Pleistocene landscape dynamics in general and glacier fluctuations in particular (Lehmkuhl et al., 2016). A general framework or pattern about the timing of the last glaciation, its maximum, the extension of the glaciers during the different time periods of the Late Pleistocene and Holocene and related altitudinal shifts of the vegetation zones are largely unknown. Some first ideas about former glaciations in the Altai were published in the late 19th century (e.g., Mihaelis, 1886). Several dozens of stratigraphic schemes for the Quaternary have been created only for the Russian Altai. These schemes were based on differing theories about the number and extent of glacial epochs. For the Late Pleistocene, for example, some authors reconstructed one glaciation (Obruchev, 1914; Svitoch and Faustov, 1978; Butvilovskiy, 1993), one glaciation with two 'megastadials' (Okishev, 1982, 2011) or two separate glaciations (Devyatkin, 1965). The problem for the creation of a comprehensive scheme for the Pleistocene and Holocene glacial fluctuations was caused by the different approaches used, the absence of numerical ages for the moraines, the incongruity of results obtained from radiocarbon and other dating techniques and the spatial discontinuity of the reconstructions. The number of radiocarbon datings is small and they mostly covered an insufficiently long time interval. The available results of luminescence dating (Sheinkman, 2002; Agatova et al., 2009; Agatova and Nepop, 2017) or cosmogenic ^{10}Be and ^{26}Al surface exposure dating (Gribenski et al., 2016; Herget et al., 2017) remain partially controversial because older glacial forms often have not been dated, which rendered their attribution to maximal glacier extents of the LGM (Last Glacial Maximum) difficult.

In the Russian Altai, the history of Pleistocene and Holocene fluctuations of the glaciers and landscape dynamics is slightly better known because the climate is more humid, thus giving rise to more finds of datable organic remains. For the Mongolian Altai, geochronological results suggest large ice advances that correlate to the marine isotope stages (MIS) 4 and 2. This is in contrast to the results obtained from the central Mongolian Khangai mountains, where ice advances additionally occurred during MIS3. During the Pleistocene, glacial equilibrium-line altitudes (ELAs) were about 500 to > 1000 m lower in the more humid portion of the Russian and western Mongolian Altai, compared to 300–600 m in the drier ranges of the eastern Mongolian Altai (Lehmkuhl et al., 2016). In large parts of the Altai, Kanghai and north-eastern Tibetan plateau permafrost induces periglacial processes. Examples from late Holocene solifluction activity in the Altai, Khangai and north-eastern Tibetan plateau show a different intensity of solifluction processes during the late Holocene and Little Ice Age (LIA) due to a decrease in temperature and higher soil humidity (Lehmkuhl et al., 2016).

The problem of the unknown number of Pleistocene glaciations, glacial fluctuations and the timing of the maximal glacial extent(s) still remain unsolved. Sheinkman (2011) dated it to 105–115 ky BP by using thermoluminescence (TL) and varve counting and referred it to MIS 5d. Several authors (Svitoch and Faustov, 1978; Borisov and Minina, 1989) dated the maximal glacial stage with 58 ± 6.7 ka BP by using TL dating in the Chagan-Uzun key area. Okishev (2011) even referred it to the interval between 58 ± 6.7 and 32 ± 4 ka BP. MIS 3 ages were given for the Chinese Altai (Xu et al., 2009) and later re-dated to the MIS 4 stage (Zhao et al., 2013). Butvilovskiy (1993) attributed the maximum stage to about 18–20 ka BP (Butvilovskiy, 1993). Recent surface exposure results (^{10}Be) gave an age for the glacial maximum at approximately 19.2 ka BP (Gribenski et al., 2016). For south-eastern Altai, most of the palaeogeographic information is related to the South-Chuya range (Agatova et al., 2012). Using radiocarbon data, Agatova et al. (2014) were able to trace former glacier fluctuations and upper tree limit variations for this part of the Altai for the last 3 ka. Glacier advances occurred between 2300 and 1700 cal BP and during the 13th – 19th century (LIA). Further to the east, the climate becomes more arid, the vegetation is sparse and findings of organic fossils are rare. Consequently, this has also restricted the database on palaeo-information. In 1988, the University of St. Petersburg started to collect palaeoglaciologic and palaeoclimatic data on the Mongun-Taiga mountain massif (eastern part of the Altai range). The main goal of this paper is to develop a chronology of glaciation and to reconstruct fluctuations of the glacial settings, climatic conditions and treeline variability in the Mongun Taiga during the Late Pleistocene and Holocene.

2. Study area

The Mongun-Taiga mountain massif is situated in the south-eastern periphery of the Russian Altai mountains (Fig. 1). It is located within the internal drainage basin of the Mongolian Great Lakes. The highest peak has an elevation of 3971 m *a.s.l.* The main ridge stretches from southwest to northeast, reaching 3000–3300 m in the western and eastern periphery and 3500–3970 m in the central part. The climate of the massif is cold and arid. According to data of the closest meteorological station Mugur-Aksy (1830 m *a.s.l.*, 50° 22′ 45″ N, 90° 26′ 0″ E; WMO code 362780: about 30 km to the north-east of the massif) the average annual precipitation is 160 mm, the mean summer temperature is 12.0 °C and mean temperature about − 3 °C. Forest vegetation is concentrated on the northern slopes of the massif with *Larix Sibirica* usually occurring between 2000 and 2400 m *a.s.l.* The upper treeline varies between 2400 m on north-western slopes to 2300 on the north-eastern slopes. The upper treeline of the north-eastern slopes corresponds to an average summer temperature of 8.8 °C (Chistyakov et al., 2012). Glacial relief forms such as cirques, U-shaped valleys or moraines are widely present at altitudes above 1800 m *a.s.l.* Three different morphological groups of moraines, representing glacial advances, can be distinguished.

Currently, there are 30 glaciers having a total area of 20.2 km^2 within the massif. Valley glaciers comprise over half of that area. The number of small hanging and cirque glaciers, however, is also significant. One large proportion of the glaciers is found around the highest summit of the massif (3971 m *a.s.l.*) and a smaller one to the west of the Tolaity valley having a maximal altitude of 3681 m *a.s.l.* The central part of both complexes is dominated by a flat summit-glacier. This type of glacier diverges radially and has a uniform accumulation zone. Usually, the largest glaciers develop on the leeward, north-eastern slopes. The ice accumulation there is the result of a combination of snow-drift and low insolation.

The vertical extension of glaciation is from 3970 to 2900 m *a.s.l.* The average ELA for the glaciers of the Mongun-Taiga massif is at 3390 m *a.s.l.* The glaciers of the massif, however, are retreating — as they are in many other parts of the world. The tendency of an accelerating retreat is particularly well-documented for the largest glaciers during the last 10 years: for example, the average rate of retreat of the Shara-Horagai glacier in 2013–2016 was 44.2 m/year (Ganiushkin et al., 2015 and unpublished results).

3. Materials and methods

The investigations are based on in situ measurements and observations (glaciologic, glacio-geomorphic, hydrological, meteorological, palaeogeographic) over the last 35 years that enabled a modelling of palaeoclimate and timing of glaciation. The glaciologic and glacio-geomorphic field observations included the delineation of the present-day glaciers using field mapping, route observations, GPS-trekking of glacial termination and moraines, a geodetic

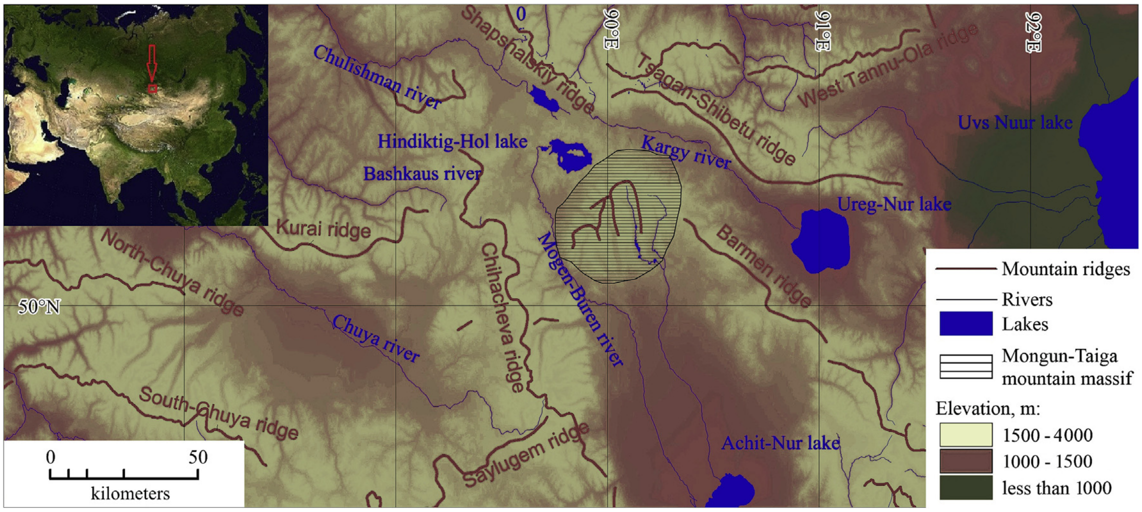

Fig. 1. Orographic map of the Mongun-Taiga massif and neighbouring mountain ranges with the insert in the upper left showing the study area on the Eurasian continent.

survey of glacial snouts and moraines, snow height measurements and duration of snow cover, evaluation of the ELA and mass balance multiannual studies.

3.1. Glacier observations

The geodetic surveys (cf. Figs. 2 and 3) were performed on the Leviy Mugur glacier and its LIA moraine (in 1994), on the snout and LIA moraines of the Shara-Horagai glacier in 1990 and 2013 and the Vostotschniy (east) Mugur in 2012. In addition, aerial photos of 1966, Landsat-7 04.09.2001, Landsat-8 12.08.2013 and Spot-5 2011-09-19 space imagery having a spatial resolution of 0.5 up to 30 m per pixel were used. Every scene was radiometrically normalised and geographically referenced using orbital parameters. An automatic and systematic geometric correction of the raster data was applied by using a mathematical model of the view angles of the satellite camera and its position at the moment of the scene collection (rigorous model). UTM/WGS 84 projection (zone 46) was applied as reference frame for georeferencing. The imagery was orthorectified using the 30 m ASTER GDEM v.2 digital elevation model (https://gdex.cr.usgs.gov/gdex/), and treated using a moderate-sharpening filter for graphic quality preservation. Processing of space imagery and aerial photographs was carried out using the photogrammetric software ERDAS Imagine.

The delineation of the glaciers and moraines was mapped manually. The minimum size of glaciers to be mapped was

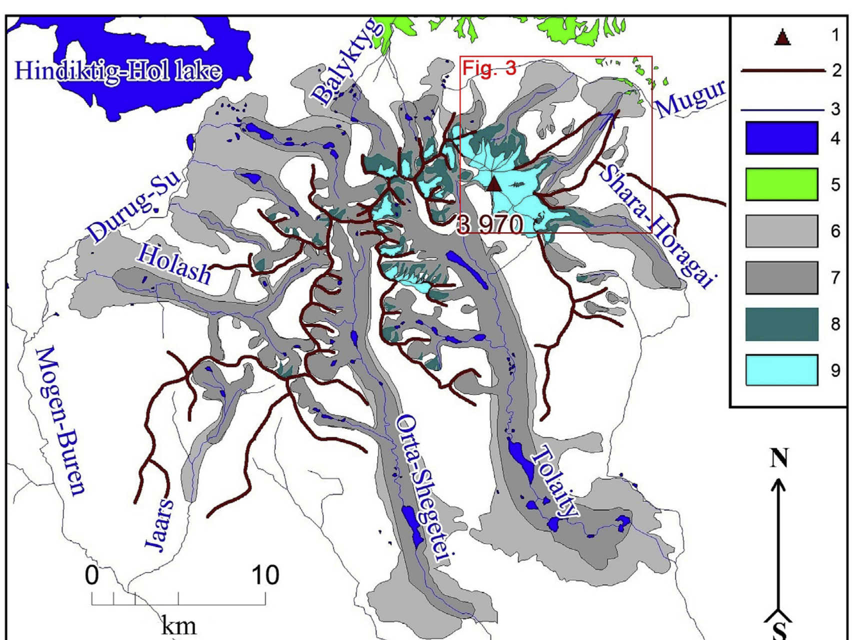

Fig. 2. Reconstruction of palaeoglaciation of the Mongun-Taiga massif. 1: main summit of the massif, 2: mountain ridges and watersheds, 3: rivers, 4: lakes, 5: forested areas, 6: hypothesised extent of glaciers during MIS 4 (based on geomorphic mapping and results given Tables 1 and 2), 7: hypothesised extent of glaciers during MIS 2 (based on geomorphic mapping and results given Tables 1 and 2), 8: LIA glaciers, 9: present-day glaciers. The red frame (inlet) refers to the area plotted in Fig. 3. (For interpretation of the references to colour in this figure legend, the reader is referred to the Web version of this article.)

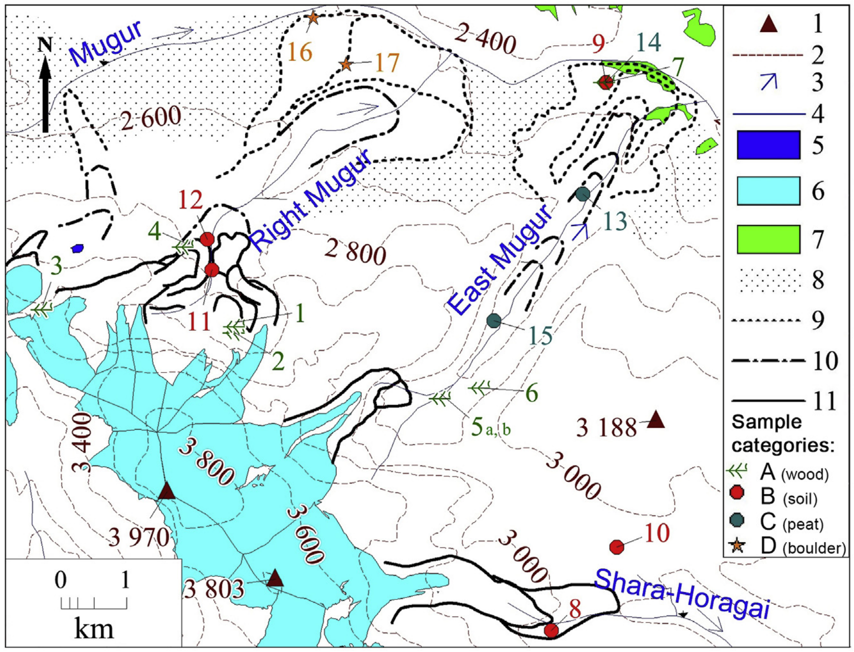

Fig. 3. Main sampling locations on the north-eastern slope of the Mongun-Taiga massif. The indices in the map correspond with those in Table 2. Topographic and geomorphic features: 1: main summits of the massif, 2: contour lines, 3: river flow direction, 4: rivers, 5: lakes, 6: present-day glaciers, 7: forested areas, 8: traces of MIS 6 (?) moraines; 9: moraines of group I (hypothesised to be deposited during MIS 4), 10: moraines of group II (hypothesised to be deposited during MIS 2), 11: moraines of group III (neoglacial). Sample categories (sampling site): A: locations of buried wood (1, 2, 3, 4, 5, 6, 7, 14), B: soils (8, 9, 10, 11, 12), C: peat (several sites: 13, 14, 15), and D: boulders.

0.01 km^2. The boundary line was mostly determined by direct observations.

3.2. Geomorphic observations and ELA determination

The following glacio-geomorphic features were mapped: cirques, riegel, troughs, trough shoulders and moraine ridges. This mapping resulted in the reconstruction of the position and margins of former glaciers. Parameterisation of the present and reconstructed glaciers was performed using topographic maps at a scale of 1:100000 and 1:25000. The determination of the present-day ELA of the Mongun-Taiga was performed by using by direct observations (position of the snow line at the end of the ablation season during several years) and satellite imagery at the end of the ablation seasons.

3.3. Meteorological and hydrological observations

Meteorological and hydrological observations included in-situ measurements of temperature, precipitation, snow-melting and runoff in the Shara-Horagai (1990, 2013; observation stations at: 50.265292°N/90.176922°E, 3130 *m a,s.l.*; 50.260703°N/90.225562°E, 2780 *m a.s.l.;* 50.261678°N/90.142461°E, 3800 *m a.s.l.*), Vostotschniy (East) Mugur (1993, 1995, 2010, 2011, 2012; observation stations at: 50.335613°N/90.225065°E, 2259 *m a.s.l.*, 50.293760°N/90.181795°E, 2668 *m a.s.l.*) and the Praviy Mugur (1994; observation stations at: 90.101288°E 50.305251°N, 3200 *m a.s.l.*, 50.320428°N/90.140287°E, 2610 *m a.s.l.*) valleys. In each case, measurements (air and ground temperature, precipitation, solar radiation, air humidity) were continuously done during the ablation season at different elevational points: close to the upper treeline; near the edges of glaciers; on glacial surfaces; on lateral moraines over the glacial snouts and on the main summit of the massif. In addition, the data of the Mugur-Aksy meteorological station were considered. Using all these datasets, a spatial extrapolation and modelling was rendered possible. The vertical temperature gradient for the average summer temperature was 0.69 °C/100 m and the pluviometric gradient was 7 mm/100 m (Chistyakov et al., 2012). In addition, a regional, empirical model (Chistyakov et al., 2012) of annual ablation (a_i; mm water equivalent per year) was obtained using the average summer temperature at ELA (t_0):

$$a_i = 36,14(t_0)^2 + 294,6t_0 + 511,6 \quad (1)$$

3.4. Numerical and relative dating of surfaces

Dating of buried wood samples, peat and soils (humus) was done using the radiocarbon technique. Peat and wood samples were cleaned using an acid-alkali-acid (AAA) treatment. ^{14}C dating was performed at the KÖPPEN-Laboratory of the Saint-Petersburg State University. Radiocarbon dating was performed by using a Quantulus 1220 liquid scintillation spectrometer (Perkin Elmer, USA). Dating of strongly-decomposed peat and humus (palaeosoils) was performed on the fraction that dissolves in hot 2% NaOH (Arslanov et al., 1993). A V_2O_5 coated $Al_2O_3 \times SiO_2$ catalyst has been employed for benzene synthesis.

The calendar ages were obtained using the OxCal 4.3 calibration program (Bronk Ramsey, 2001, 2009) based on the IntCal 13 calibration curve (Reimer et al., 2013). Calibrated ages are given in the 1σ range (minimum and maximum value for each). If not otherwise mentioned in the text, calibrated years BP (cal BP) are used.

Furthermore, we tried to derive numeric age estimates for two end-moraines by dating rock boulders using ^{10}Be. However, the suitability of rock boulders was very limited. Two small boulders (c. 0.3 m in height) were sampled and analysed for in situ ^{10}Be. We were aware that the obtained ages would only be indicative (if that). The rock samples were pre-treated following the standard procedures. Samples were crushed and sieved and the quartz isolated by treating the 0.25 mm−0.6 mm fraction with *aqua regia* to destroy organic contaminations and any calcareous components.

After a 1 h treatment with 0.4% HF, we used a floatation system to physically separate feldspar and mica components from the quartz. Remaining remnants of these were removed by repeated 4% HF leaching steps. Once pure quartz was obtained, we added a ^{9}Be-carrier solution and dissolved the samples in 40% HF. Be was isolated using anion and cation exchange columns followed by selective pH precipitation techniques (von Blanckenburg et al., 1996). The Be hydroxides were precipitated, dried, and calcinated for 2 h at 850 °C to BeO. The $^{10}Be/^{9}Be$ ratios were measured at the ETH Laboratory Ion Beam Physics' Accelerator Mass Spectrometry (AMS) facility using the ^{10}Be standard S2007N with a nominal value of $^{10}Be/^{9}Be = 28.1 \times 10^{-12}$ (Kubik and Christl, 2010; Christl et al., 2013). S2007N has been calibrated to the ^{10}Be standard ICN 01-5-1 of K. Nishiizumi and has a nominal $^{10}Be/^{9}Be$ value of 2.709×10^{-11} (Nishiizumi et al., 2007). The 1σ error of S2007N is 2.7% (Christl et al., 2013). Measured $^{10}Be/^{9}Be$ ratios were corrected for ^{10}Be contributed by the Be-carrier (blank value: 0.003E-12). ^{10}Be exposure ages were calculated using CRONUS-Earth (http://hess.ess.washington.edu/math/) version 2.3 with a ^{10}Be production rate of 4.01 ^{10}Be atoms/g SiO_2/year (Borchers et al., 2016) and a ^{10}Be half-life of 1.387 ± 0.012 Ma (Korschinek et al., 2010). The production rate was corrected for latitude and altitude using the scaling scheme of Stone (2000) and corrected for sample thickness assuming an exponential depth profile (Brown et al., 1992) having an effective radiation attenuation length of 160 g cm^{-2} (Gosse and Phillips, 2001) and a rock density of 2.65 g cm^{-3}. Effects of variations of the geomagnetic field on the ^{10}Be age are said to be negligible (Masarik et al., 2001; Pigati and Lifton, 2004).

In addition, relative-dating techniques were used to delineate a chronology of geomorphic deposits, e.g., moraines. These techniques primarily are based on weathering patterns. On a polygon (moraine) having an area of 10 m^2, boulders having a diameter over 30 cm were marked and counted. Then properties were measured that included the occurrence of shear-strained boulders (C, %), the degree of embedment into finely-grained material (B, %), weathering rind measurements (W, mm), lichen coverage (L, %), the number of boulders having a diameter over 30 cm (N), rock surface hardness (R) and the proportion of flat-topped boulders (F, %). The rock surface hardness was measured using a Schmidt hammer, which measures the rebound value of a boulder (Matthews and Shakesby, 1984; Goudie, 2006; Shakesby et al., 2006) and is a portable instrument originally developed to test concrete quality in a non-destructive way (Schmidt, 1951). A spring-loaded bolt impacting a surface yields a rebound- or R-value, which is proportional to the hardness (compressive strength) of the rock surface. Applied in geomorphology, more-weathered surfaces provide low R-values and less-weathered surfaces correspondingly high R-values (Böhlert et al., 2011). We used an N-type Schmidt hammer. Three measurements were done for each boulder (5 when there were larger differences between individual measurements) and then the average value was registered. Measurements were carried out in the valleys of the upper tributaries of the Mugur river on the north-eastern slope of the Mongun-Taiga massif at 19 sites where about 2500 boulders were described and analysed.

3.5. ELA and palaeoclimate modelling

Modelling of palaeotemperature, palaeoprecipitation and ELA was done using the approach of Ganyushkin (2015) and Glazyrin (1985) according to which the mass balance (M) of a glacier at a given altitude Z close to Z_0 (ELA) is the following:

$$M(Z) = M(Z_0) + E\Delta Z \tag{2}$$

where E = energy of glacierisation (activity index or the mass-balance gradient at the ELA; IACS, 2011), $\Delta Z = Z - Z_0$. In case of changes of precipitation and temperature, the mass balance at the altitude of interest can be calculated as:

$$M(Z) = P \cdot c(Z_0) - a(T(Z_0) + \Delta T)) + E_n \Delta Z \tag{3}$$

where $c(Z_0)$ = present accumulation at the ELA; P = ratio of past annual precipitation to present-day situation; T = mean summer temperature; a = ablation; $a(T(Z_0) + \Delta T)$ = ablation at the present-day ELA in case of a change of the average summer temperature ΔT; E_n = energy of glacierisation (activity index) under new climatic conditions.

The altitude, where under the new climatic conditions the annual mass balance $M = 0$, corresponds to the *new ELA* (Z_{0n}):

$$P \cdot c\left(Z_f\right) - a(T(Z_0) + \Delta T)) + E_n(Z_{0n} - \Delta Z_0) = 0 \tag{4}$$

Consequently, changes of the ELA (**$\Delta Z_0 = Z_{0n} - Z_0$**) are given by:

$$\Delta Z_0 = -(P \cdot c(Z_0) - a(T(Z_0) + \Delta T))/(E_n) \tag{5}$$

The ablation at the ELA is calculated using the extrapolated data from the Mugur-Aksy meteorological station temperature (gradient 0.69 °C/100 m; cf. Equation (1)). At the ELA, ablation equals accumulation. The energy of glaciation (E_n) can then be calculated by

$$E = PK(\Delta p/\Delta Z) + \Delta a/\Delta Z \tag{6}$$

where K = coefficient of snow concentration (at ELA $K = a/p$), p = average annual precipitation at ELA, $\Delta p/\Delta Z$ = gradient of precipitation, $\Delta a/\Delta Z$ = gradient of ablation.

Equation (5) contains 3 variables: ΔZ_0, P, ΔT. The first of them can be derived from palaeoglacial reconstructions. The reconstruction of the ELA was done using the method proposed by Kurowsky (1891):

$$z_{0n} = (z_0 S + \Delta S(z_1 + z_2)/2)/(S + \Delta S) \tag{7}$$

where z_{fn} = reconstructed ELA, ΔS = difference between the area of the palaeoglacier and its present-day area, z_1 = present-day altitude of the glacial snout and z_2 = altitude of the palaeoglacial snout.

With an estimation of ΔZ_0 for the reconstructed glaciers, Equation (5) can be used to determine P (if we know ΔT) and ΔT (if P is known). Using this approach, scenarios can be calculated by assigning a value to one of the unknown parameters. The choice of probable scenarios can be done on the basis on regional palaeoclimatic reconstructions or on regional statistical correlations between precipitation and temperature. In the south-eastern Altai, a clear correlation between summer precipitation and average summer temperature can be derived (based on meteorological stations of the Altai (Ganyushkin, 2015). This can be expressed by the following empirical equation:

$$\Delta T = 2.245 \ln P - 0.9779 \tag{8}$$

Another possibility is to use the correlation of monthly precipitation with monthly temperature from the closest meteorological station Mugur-Aksy to Mongun-Taiga massif (Ganyushkin, 2015). The empirical relationship looks as follows:

$$P = 0.6635e^{0.0748\Delta T} \tag{9}$$

By combining Equation (5) with (8) and (9), temperature and precipitation differences to the present-day situation can be calculated. This procedure has been applied to reconstruct palaeotemperatures and palaeoprecipitation. If the values of P or ΔT for some time point are, however, known from literature, calculations were directly carried out using Equation (5). Having the ΔT value, the difference between the present-day and the past upper treeline ΔF can be calculated. Finds of buried wood gave, in addition, indications about the past upper treeline. Assuming that the found wood was close to the treeline, then $\Delta T = \Delta F/G_t$, with ΔF = difference between the altitude of the find and the altitude of the current treeline, G_t = present-day altitudinal gradient of temperature.

The obtained ΔZ_0 and values of ELA and treeline variations should be corrected for tectonic shifts. In several parts, the Altai mountains are tectonically very active. This activity led to the dislocations of quaternary sediments (e.g., the northern bank of the upper flow of Shara-Horagai). Recent earthquakes having a magnitude of 7–8 took place in the area of the Mongun-Taiga massif (Actit-Nur earthquake 19th of October 1938 and Ureg-Nur earthquake 15th of May 1970). Tectonic movements during the Late Pleistocene are indicated by indirect traces, e.g. the presence of faults with a vertical amplitude of up to 500 m (near the river Shara-Horagay), the occurrence of hanging valleys (300–400 m), or the presence of post-glacial erosional trenches with a depth of up to 500 m. From this the tectonic uplift can be roughly estimated with about 400 m for the last 75 ka. This corresponds to an uplift rate of about 5.3 mm/year.

4. Results

4.1. Geomorphic patterns and glacier extension

The first group (group I) of moraines is composed of a bluish-grey sandy material, having a large number of rounded boulders, mostly granite. Its surface is hummocky-like, with many small, round thermokarst depressions and lakes. These forms are located at the transition from U-shaped valleys to the intermountain depressions, i.e. at altitudes of 1800–2200 m *a.s.l.* In some valleys, these moraines can be traced on trough shoulders until the cirques (at an altitude of about 3100 m *a.s.l.*). Furthermore, these moraines can be subdivided into several stages: the oldest holds the greatest area but, in some places, the terminal moraines of the youngest stage break through the older ones. The moraines of group II are situated within the troughs, reaching 2100–2200 m *a.s.l.* at their lowest extension. Their composition is similar to the first group. These are typical moraines of a valley glaciation. The moraines show erosion in many places. Some moraines still dam lakes in the tongue basin, especially the youngest of these moraines. Lateral moraines of this group can be traced on trough shoulders up to the cirques to an altitude of about 2600–2700 m *a.s.l.*, but 50–150 m below the previous group. The moraines of group III are characterised by coarse angular stony material intersected with sand and clay deposits. These types of moraines exhibit 3 stages that are usually adjacent to each other or even overlap each other. They mostly form sediment complexes in the upper part of troughs next to the present-day glaciers. These moraine complexes are usually bare of vegetation or slightly covered by pioneer vegetation; they have steep fronts. Glacial ice is sometimes exposed by thermokarst. These moraines are almost unaffected by erosion.

Although nowadays the glaciers mostly have a north-eastern aspect, the ancient moraines are more extensive on the southern slopes of the massif (Fig. 2). According to our reconstruction, the glaciers of the southern and south-eastern slopes had a length of up to 30–35 km during the LGM, while on the northern slopes they had a length less than half of that. At the same time, the glacial termini were 300–400 m lower on the southern slopes than on the northern slopes. Such a disproportion could only have been caused by a higher moisture flux from the south and/or due to snow drifting from the north-facing slopes.

4.2. Dating of surfaces

4.2.1. Relative chronology

The results of relative dating are given in Table 1. Both variables, shear-strained boulders (C) and their embedment into the finely-grained material (B), increase proportionally along the morphological groups of moraines (increasing values from III to I; Table 1). Also, the proportion of flat-topped boulders (F) increases in the same order. The rebound values and the weathering rind thicknesses show that the surface of the moraine groups I and II were the most weathered. From a stratigraphic point of view, moraine group I must be older than moraine group II. This trend is best reflected by the parameters C, B and F. This means that the cracking of larger boulders and their embedment into the fine material are suitable processes to describe the long-term evolution of moraines. The disintegration of smaller boulders on moraine surfaces or their progressive coverage by finer sediments and soils, the coverage of the boulders with lichens and the flattening of the large boulders are active processes at the early stage of moraine evolution. Rebound values (R) rapidly decreased during the early stage of moraine evolution. The slight increase of these values for the oldest moraine group could have been caused by the disintegration of less solid boulders and the preservation of the more resistant part. Chemical weathering (oxidation, ferruginisation) in conditions with low precipitation strongly depends on local differences in moisture content. Usually, slightly thicker weathering rinds were measured near creeks (higher air humidity; in general 1–2 mm thicker weathering rinds compared to drier conditions; data not shown). This might have slightly biased the temporal trend of weathering rind thickness.

4.2.2. Radiometric chronology

Direct dating of the moraines was difficult. Dating of warm periods during interstadials can help to fix glacial advances to a time interval. The minimal age for the warm period after the advance of the earliest stage of the third moraine group (3141–2776 cal BP; Table 2) was measured in the Praviy (right) Mugur valley (soil on the surface of a grass-covered moraine, adjacent to a younger bare moraine complex, index 11 in Fig. 3 and Table 2). There is also a high probability that the buried wood having an age 3697–3495 cal BP (index 7; Fig. 3), and found about 50 m above the present-day upper treeline, refers to this warm phase. Another time marker is a buried soil having an age of 5881–5326 cal BP (index 8; Table 2, Fig. 3) that was found in the Shara-Horagai valley where the river cuts a moraine. This means that one (or maybe two) glacial advance(s) occurred between 5.5 and 3.6 ka cal BP. This period can be referred to the earliest glacial advance of the Neoglacial period (cooling period that started after the Holocene Climatic Optimum, Akkem stage of Altai glaciers). A warmer period obviously ended about 1.2 ka BP indicated by a buried soil (1293–1089 cal BP; index 12 in Fig. 3) and peat (1224–1009 cal BP; buried by stony material from a talus cone, index 15 in Fig. 3). The maximum advance of the LIA glaciers was about 1810–1820 AD (Ganiushkin et al., 2015) according to dendrochronological measurements.

The warm period preceding the Neoglacial was characterised by a rise of the upper treeline to a level of 300–400 m higher than today. Several finds of ancient wood having 10180–10580 (sample site 5; Fig. 3), 9245–9000 (sample site 6) and 6350–6170 cal BP (sample site 5; Table 2) indicate this shift. The dating of peat, wood and charcoal (Table 2 and Fig. 3; sample sites 13, 14, 15) indicates that relatively warm and/or moist conditions seem to have existed in the mid-Holocene. According to fossil wood finds having an age of 31436–31178 and 29537–28759 cal BP (sample sites 3 and 4; Table 2) at altitudes of 1000 and 500 m above the current upper

Table 1
Relative dating of moraines of the Mongun-Taiga massif. I, II, III correspond to the morphological moraine groups (Fig. 3).

Moraine group	Number of polygons	N_1/N_2 [a]	C, % [b]	B, % [c]	R [d]	W, mm [e]	F, % [f]	L, % [g]
I	5	0.20	13.9	73.7 ± 2.50	44.7 ± 1.63	7.0	33.2	56.8
II	5	0.33	7.0	66.3 ± 1.83	40.4 ± 1.80	10.3	32.1	79.2
III	9	0.03	3.3	49.3 ± 1.57	51.3 ± 2.62	4.8	3.7	29.0

[a] N_1 = the number of boulders having a diameter over 30 cm, N_2 = number of smaller boulders and cobbles.
[b] C = shear-strained boulders; area coverage in %.
[c] B = embedment into finely-grained material.
[d] R = rebound value (Schmidt-hammer); ±standard error; n (total) = 3708 (110, 229, 3369).
[e] W = weathering rind thickness (W, mm); ±standard error; n (total) = 76 (10, 15, 51).
[f] F = proportion of flat-topped boulders.
[g] L = lichen coverage (area coverage given in %).

Table 2
Radiocarbon data from the Mongun-Taiga massif.

Sampling site (cf. Fig. 3)	Laboratory ID	Altitude (m)	Material (cf. Fig. 3)	^{14}C age ± error	Calibrated age (1σ), cal BP	Climate interpretation	Source
1	LU-3666	2915	wood (A)	57810 ± (≥1820)	c. 60000–56000	warm	this paper
2	LU-5822	2965	wood (A)	39300 ± 700	43688–42567	warm	this paper
3	KI-912	3300	wood (A)	27500 ± 180	31436–31178	warm	(Revushkin, 1974) [a]
4	KI-913	2800	wood (A)	25100 ± 160	29537–28759	warm	(Revushkin, 1974) [a]
5	SOAN 8116	2700	wood (A)	–	10580–10180 [b]	warm, humid	(Nazarov et al., 2012)
6	LU-6949	2640	wood (A)	8140 ± 80	9245–9000	warm	this paper
5	SOAN 8117	2700	wood (A)	–	6350–6170 [c]	warm, humid	(Nazarov et al., 2012)
13	LU-3219	2460	peat (C)	4920 ± 80	5740–5588	humid	this paper
8	LU-7283	2960	soil (B)	4860 ± 190	5881–5326	warm	this paper
9	LU-5830	2350	charcoal in soil (B)	4570 ± 80	5445–5054	warm	this paper
14	LU-6451	2350	peat (C)	4110 ± 100	4819–4522	humid	this paper
10	LU-7284	2855	soil (B)	3580 ± 280	4290–3515	warm	this paper
7	LU-6452	2350	wood (A)	3370 ± 70	3697–3495	warm, humid	this paper
11	LU-8382	2675	soil (B)	2820 ± 150	3141–2776	warm	this paper
12	LU-6818	2630	soil (B)	1280 ± 80	1293–1089	warm	this paper
15	LU-6817	2535	peat (C)	1190 ± 60	1224–1009	warm, moist	this paper

[a] A δ^{13}C correction was at that time not performed. A δ^{13}C value of −25‰ was assumed for the correction of the ^{14}C data.
[b] Original data 10380 ± 200 cal BP.
[c] Original data 6260 ± 90 cal BP.

treeline, another warm period seems to have existed even before the Last Glacial Maximum (LGM). Such a rise of the treeline must have been accompanied by a drastic reduction of the glaciers to a length smaller than the present-day situation. The moraines of group II most likely refer to the period between about 10 and 29 ka cal BP and, therefore, correspond to MIS 2 (see below). The ancient wood remains (28.7–31.4 ka cal BP) are probably part of the MIS 3 warm period. There are several other finds of buried trunks of *Larix Sibirica* (Fig. 4) having an age of 43 to about 60 ka cal BP that can be found 600 m higher than the present-day upper treeline (sample sites 1 and 2, Table 2; Fig. 3) that support this hypothesis. Voelker and workshop participants (2002) dated MIS 3 to between 59 and 29 ka BP and Pettitt and White (2012) to between 59 and 24 ka BP. The moraines of group I were deposited before MIS 3 and, therefore, correspond to MIS 4 or older (Fig. 3).

Although the obtained ^{10}Be ages of the moraine boulders would fit with an LGM around 24 ka and a stage of the Youngest Dryas (Table 3), the ages seem to be too young. The age (moraine group II) of these boulders does not fit with their topographic and geomorphic position (moraine group I). Either the moraine groups II and I are very close together (where the boulder samples were taken; but then the geomorphic map would have to be reconsidered) and consequently are difficult to be discerned separately or the obtained ages are biased due to an exhumation of the boulders over time. Both possibilities are likely — however, the likelihood of boulder exhumation is in this permafrost-overprinted region higher (and thus, the measured ages too young). The height of the boulders (30–40 cm) was unfortunately very low and, consequently, disturbances may have occurred.

Fig. 4. Trunk of a *Larix Sibirica* (category A (buried wood), site 2 (LU-3666) in Fig. 3) having an age (1-σ range) of 43688–42567 cal BP (photo by authors, 1999).

4.3. Palaeoclimate-modelling and ELA reconstructions

During the maximal stage, the total area of glacier cover of the massif was 516 km^2. The maximum advance of the glaciers

Table 3
Sample properties and ^{10}Be surface ages. Latitude and longitude are in WGS84 coordinates. Shielding correction includes the effects caused by mountain topography, dip and strike of the various boulder surfaces.

Sample name	ETH/UZH label	Latitude (DD)	Longitude (DD)	Elevation (m *a.s.l.*)	Thickness (cm)	Shielding factor	Quartz (g)	Carrier (mg)	^{10}Be content[a] (atoms g^{-1})	Uncertainty ^{10}Be content [b] (atoms g^{-1})	Exposure age[c,e] (a)	Uncertainty[d,e] (+/− a)
16	MIS2	50.337	90.162	2500	3	0.983	20.61	0.35	3.35E+05	1.42E+04	11229	1083 (482)
17	MIS4	50.343	90.154	2408	3	0.947	26.17	0.349	6.33E+05	2.63E+04	23633	2306 (1014)

[a] We used a density of[a]2.65 g cm^{-3} for all samples.
[b] Uncertainty includes AMS measurements errors and statistical counting error.
[c] We used a rock erosion rate of 1mm/ka.
[d] External (internal) uncertainty.
[e] Surface exposure ages were calculated with the CRONUS-Earth online calculators (http://hess.ess.washington.edu/, Balco et al., 2008 and version 2.3) and using the scaling scheme for spallation based on Lal (1991)/Stone (2000).

probably occurred about 75 ka ago (end of MIS 5a, beginning of MIS4) when an abrupt cooling (about 12 °C) caused the onset of the last glacial period in Tibet (neighbouring region) according to ice-core records (Thompson, 1997; Shi et al., 2008). We assumed a tectonic uplift rate of about 5.3 mm/year for the correction of the palaeotopography (Table 4). The glaciers moved from the troughs to the flat piedmonts and joined each other at the piedmont of the mountains (Fig. 2). The average ELA depression ΔZ_0 for this stage was about 800 m. Based on our results (Tables 2 and 4), the reconstructed glaciated area was 342 km^2 during the second stage of MIS 4 (moraine group I). During the third stage of MIS 4, the glaciated area was similar. Some of the glaciers even overlapped the moraines of the maximal stage (1790 m *a.s.l.* in the Orta-Shegetei valley). These small stages could be differentiated from a topographical and geomorphological point of view.

During the MIS 2 maximum (moraine group II), the glacial area was about 318 km^2. Valley glaciers prevailed. The aspect asymmetry of glaciation was similar to that of MIS 4. The average ELA depression was about 660 m. In each of the subsequent 4 stages, the glaciated area was lower than that of the previous stage (Table 4).

Table 4
Reconstruction of the vertical fluctuation of the upper treeline ΔF (ΔF^* with tectonic corrections), ELA depression ΔZ_0 ($\Delta Z_0{}^*$ with tectonic correction), precipitation *P%* (*% of the present-day situation*) and temperature difference to the present-day situation ΔT.

Period (and ages of samples of Table 2)	ΔF (m)	ΔF^* (m)	ΔZ_0 (m)	$\Delta Z_0{}^*$ (m)	*P%*	ΔT °C
MIS 4						
MIS 4 maximum		− 390	− 800	− 1200	210	− 2.7
MIS 4 stage 2		− 505	− 790	− 1163	105	− 3.5
MIS 4 stage 3		− 465	− 790	− 1145	95	− 3.2
MIS 3						
56000–60000 cal BP	615	309	–	245	100	2.1
43688–42567 cal BP	665	470	–	332	100	3.0
31436–31178 cal BP	1000	854?	–	458	200	5.9 ?
29537–28759 cal BP	500	356	–	102	200	2.5
MIS 2						
MIS 2 maximum		− 550	658	− 758	46	− 3.8
MIS 2 stage 2		− 536	643	− 731	46	− 3.7
MIS 2 stage 3		− 507	578	− 655	43	− 3.5
MIS 2 stage 4		− 493	523	− 594	43	− 3.4
MIS 2 stage 5		− 478	485	− 551	46	− 3.3
Holocene						
10580–10180 cal BP	400	345	–	84	200	2.4
9245–9000 cal BP	340	292		37	200	2.0
6350–6170 cal BP	400	367	–	98	200	2.5
5881–5326 cal BP		22	–	21	100	0.15
Akkem stage 5326–3697 cal BP	–	− 145	151	− 174	110	− 1.0
3697–3495 cal BP	50	31	–	2	110	0.2
Historical stage 3495–1293 cal BP		− 58	120	− 129	119	− 0.4
1293–1009 cal BP		0	0	0	100	0
LIA 1810–1820 AD		− 188	120	− 121	73	− 1.3

5. Discussion

5.1. Climate and treeline variability during the Late Pleistocene

According to the topographic position of the observed moraines, we assume that the maximum glacier advance occurred during MIS 4. This would agree with Zhao et al. (2013) who also dated the maximum glacial extension in the Chinese Altai to MIS 4. Surface exposure dating resulted in an estimated age of about 24 ka, but this result seems questionable. For the exposure date to represent the true formation or abandonment age of the landform as closely as possible, the sampled object (boulder, clasts or bedrock) surface must have i) undergone single-stage exposure (no pre-exposure/inheritance); ii) been continuously exposed in the same position (not shifted); iii) never been covered and iv) undergone only minimal surface weathering or erosion (not spalled) (Ivy-Ochs and Kober, 2008). The dated boulders would appear probably to have been exhumated and consequently do not match point iii). Data of the Gulia glacier show that the lowest temperatures during MIS 4 occurred c. 70 ka BP. Thereafter, temperature gradually increased until 57 ka BP and the beginning of MIS 3. The coldest period was accompanied by a higher aridity, a decrease of the forest vegetation and a rapid (2–2.5 times quicker) increase in dust accumulation on glaciers (Klinge, 2001; Shi et al., 2008). We therefore suggest that the maximal glacial advance in the Mongun-Taiga massif happened about 75 ka BP (Fig. 5). Devyatkin (1981) and Murzaeva et al. (1984) calculated that annual precipitation was during MIS 4 1.5–3 times higher in the Mongolian Great Lake Depression. Based on pollen analyses from the north-western Altai (Anui dva), Malaeva (1995) estimated a precipitation rate of about 400–700 mm/a. The topographic asymmetry of glaciation is noteworthy and indicates that the southern slopes accumulated a larger amount of snow (and therefore had either more precipitation or very substantial additions due to wind drift).

As the glaciers advanced worldwide and the global climate became colder, the oceans cooled down c. 72 ka ago (Ruddiman and McIntyre, 1981). The temperature contrasts between the continents and the oceans decreased, but the temperature contrasts between the poles and the equator grew. That led to an increased meridional circulation, blocking the zonal atmospheric transfer and terminated glacial growth in continental mid-latitude areas, although the minimum temperatures ($\Delta T = -3.5$ °C, Table 4, Fig. 4) probably occurred about 70 ka BP. Under these conditions, the upper treeline was at about 1500–1600 m *a.s.l.*, and the probability was low that a forest vegetation existed in the Mongun-Taiga massif.

MIS 3 is generally considered to have been a warmer period than MIS 4 or MIS 2 period (Van Meerbeeck et al., 2008). However, there

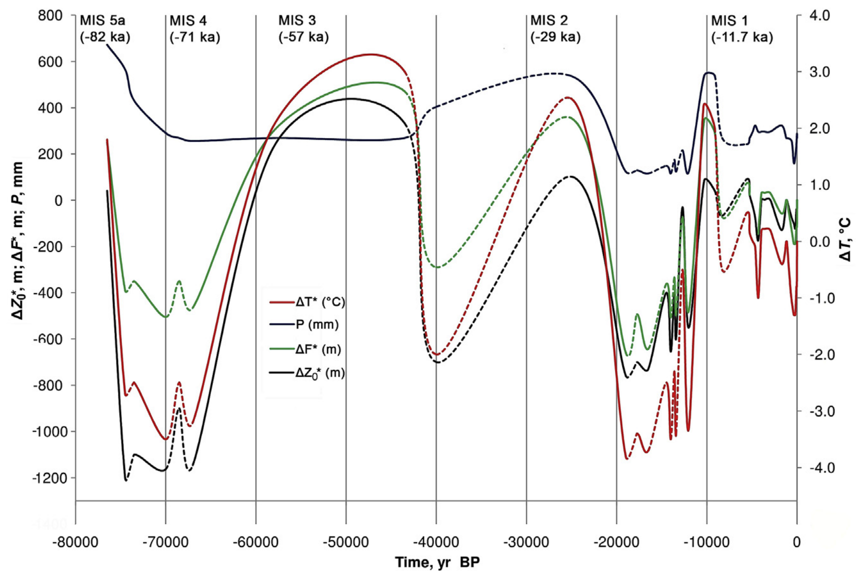

Fig. 5. Reconstruction of temperature fluctuations, precipitation, ELA and the elevation of the upper treeline (with corrections for tectonic uplift). Red line: temperature, relative to the present-day climate ΔT^* (°C); Blue line: precipitation at the current ELA, P (mm); Green line: upper treeline, ΔF^* (m) (relative to present-day elevation); Black line: ELA, ΔZ_0^* (m) relative to present-day level. (For interpretation of the references to colour in this figure legend, the reader is referred to the Web version of this article.)

is evidence of some considerable climatic fluctuations within the MIS 3 (Shi et al., 2008). According to our reconstruction for the interval of about 58–43.5 ka BP, ΔT in the Mongun-Taiga massif reached +2.1 to +3.0 °C (Table 4). This is in agreement with the reconstructions of the Gulia glacial kerns in Tibet (Shi et al., 2008), according to which the early MIS 3 (60–54 ka BP) was about 3°C warmer than today. Nonetheless, some glacier advances also occurred during MIS 3: e.g., in the Northern and Eastern Tibet (between 41 and 49 ka ago; Lehmkuhl and Liu, 1994). In the Khangai mountains the MIS 3 glacial advance (40–35 ka ago) is even considered as the largest (Rother et al., 2014). Also for the Altai region, the situation does not seem that clear. In the Kanan basin, the same moraines for a maximum glacier advance gave differing ages (Xu et al., 2009). It is, therefore, unclear if a further glacial advance occurred in the Mongun-Taiga massif in MIS 3. Several finds of ancient wood indicate a rather warmer climate. We therefore suggest that if any glacier advance took place, then it is more likely that it took place during the interval 43.5–27 ka ago and was less distinct than the MIS 4 and MIS 2 advances (Fig. 5).

There are no palaeoecological reconstructions that allow an estimation of the precipitation rates in the Mongun-Taiga massif for the period 58–43.5 ka BP. If precipitation was less than today, a further expansion of forest in that period seems unlikely. The thermic contrasts between the poles and the equator in that period were similar when compared to the present-day situation (Sergin and Sergin, 1978). The reconstructed ΔZ_0 for the time interval 58–43.5 ka BP (245–332 m; Table 4) was not large enough to suggest that the glaciers of the Mongun-Taiga massif disappeared completely. The climate during the MIS 3a stage in Tibet and north-western China was 2–4°C warmer than today with a precipitation rate of 40–100% that of the present-day (Shi et al., 2008). The finds of buried wood having an age 25–27 ka in the Mongun-Taiga massif (Revushkin, 1974) indicate that there were warm and moist conditions just before the onset of the MIS 2 glaciation. However, the altitude of the first sample (3300 m *a.s.l.*), that has a ^{14}C age of 27.5 ± 0.180 ka BP is doubtful. The place of sampling was described as a moraine ridge of one of the latest glacial advances on the left side of the outlets of the Mugur river; but in fact all moraines there are located several hundred metres lower. Therefore, this find indicates warm conditions, but the reconstructed palaeotemperatures are not particularly reliable. The altitude of the second find (29537–28759 cal BP) at 2800 m *a.s.l.* seems more reliable. Consequently, the palaeo-reconstructions are based on this sample. We calculated for that period a doubling of the annual precipitation which is in agreement with reconstructions of Murzaeva et al. (1984) and Malaeva (1995) for the Mongolian Great Lakes depression. Under such conditions the reconstructed ΔZ_0 is only about 100 m and the glacial cover would have been only slightly smaller than today.

The minimum summer insolation for 45° N was reached about 24–22 ka ago (Clark et al., 2009). The exact timing of the maximal glacier advance is large and varies from about 13 ka (Okishev, 2011) to 28–19 ka BP (Lehmkuhl et al., 2007). In southern Siberia, the summer temperatures during the LGM were about 4°C lower than today (Borzenkova, 1992) and in Tibet about 5°C lower (Shi et al., 2008). Okishev (2011) calculated a decrease in summer temperature of 3.8°C which agrees with our estimation of $\Delta T = -3.8$°C (Table 4). Sheinkman (2011) assumed that the glaciation in the Siberian mountains was mainly caused by cooling, because the ice sheets of north-western Eurasia intercepted the Atlantic moisture. The altitudinal shift of the ELA varies in literature from − 1200 m (Butvilovskiy, 1993) to − 610 m (Okishev, 2011) owing to different palaeoglacial reconstructions. Our calculations of ΔZ_0 for the MIS 2 maximum (−658 m) and the information about the increased aridity in the Mongolian Great Lakes basin let us assume that during the maximum and postmaximal stages of MIS 2 precipitation decreased (the calculated P values are in the range 43–46%; Table 4). The cooling was most pronounced (− 3.8 °C) in the Late Pleistocene (MIS2 maximum, Table 4). If we assume a MIS 2 age of the LGM (assuming that the ^{10}Be data are correct) then the calculated aridity and cooling would be even more distinct with 37% and − 4.2 °C, respectively.

5.2. Climate and treeline variability during the Holocene

The discovered *Pinus Sibirica* trees trunks of the Vostotschniy (East) Mugur valley in the Mongun-Taiga massif at an altitude of 2700 m have an age of 10180–10580 cal BP (SOAN 8116) and 6170–6350 cal BP (SOAN- 8117; Nazarov et al., 2012, Table 2).

Nowadays, the nearest *Pinus Sibirica* stands are located 150–200 km to the west and 100 km to the north of the finding site. This indicates that the amount of precipitation was higher than today and would agree with the findings of Blyakharchuk (2008). Our find of an ancient wood having an age of 9245–9000 cal BP (Table 2) in the same valley at an altitude of 2640 m *a.s.l.* refers to the same warm and moist period. This is in agreement with findings of other alpine areas such as the European Alps where the treeline was higher between about 10 and 4 ka BP mostly due to a warmer climate (Körner, 2012). The reconstructed ΔT values (2.0–2.4 °C), the doubling of precipitations (Table 4) and a 37–84 m rise of the ELA indicate that the reconstructed area of glaciation was only 1–2 km^2 smaller than today. Warmer and moister conditions than today are indicated by a find of wood (*Pinus Sibirica*) having an age of 6170–6350 cal BP (Table 2) that was discovered about 400 m higher than the present-day treeline (Nazarov et al., 2012). In contrast to this, drier conditions — leading to a forest decline (Rudaya et al., 2009) — were reconstructed for Mongolia between 7.11 and 4.39 ka (Peck et al., 2002) and in the Uvs Nuur depression (about 5 ka ago; Dorofeyuk and Tarasov, 1998; Grunert et al., 2000). For the mid-Holocene, ΔT is estimated from 2 °C (Borzenkova, 1984) to 0.5 °C (Velichko et al., 2009) in south-western to north-western Siberia and in the Altai. This matches well with our reconstructions. Charcoal finds (5445–5054 cal BP; Table 2) above the present-day treeline and a buried soil as a result of the first neoglacial advance (5881–5326 cal BP; Table 2) point to this warm period. We cannot exclude the possibility of a complete deglaciation of the massif during the late MIS 2 and early Holocene, although we have no evidence for this. A complete deglaciation seems to have occurred in the Mongolian Altai about 6 ka ago (Herren et al., 2013).

During the late Holocene, three glacial advances are usually distinguished in the Russian Altai: the Akkem stage, the 'Historical stage' and the Aktru stage (= LIA), which are considered either as phases of the Last Glacial Epoch (Okishev, 2011) or as advances of glaciers that regenerated after the Holocene thermal optimum (Neoglacial; (Solomina, 1999; Agatova et al., 2012). The Akkem stage is dated to 4.3–4.0 ka BP (Galakhov et al., 2005), 4.4 ka BP (Okishev, 2011) and 4.9–4.2 cal BP (Agatova et al., 2012). This is in general agreement with our findings. According to our ^{14}C dating (Table 2), a Neoglacial advance seemed to have occurred between 5.9 and 3.7 cal BP. The reconstructed average of $\Delta Z_0 = -151$ m and $\Delta Z_0{}^* = -174$ m do, however, not agree with Okishev (2011) who calculated 250–290 m for the different areas of the Russian Altai. This may be due to the different methods used. The approach used by Okishev (2011) may produce better results for valley glaciers but not for smaller cirque glaciers and flat-summit glaciers.

Most studies noted a change from arid to moister conditions at the transition from the Middle Holocene to the Neoglacial. According to Peck et al. (2002) the severest arid conditions in North Central Mongolia were between 7110 and 6260 cal BP, less arid conditions between 6260 and 4390 cal BP, generally humid conditions after 4390 cal BP that was then followed by a more humid climate of 2710–1260 cal BP than today. In the Minusinsk and the Uyuk depressions in northern Tuva (Dirksen and van Geel, 2004) the climate became more humid 4–3 ka BP. About 3 ka BP annual precipitation increased under relatively cold conditions (until 1.6 ka BP). A moderately comparable trend was detected in the Uvs Nuur depression by Dorofeyuk and Tarasov (1998) and Grunert et al. (2000). Based on the temperature decrease ($\Delta T = -1$ °C), we obtained a precipitation rate that slightly exceeds the present-day situation ($P = 110\%$). This agrees well with the increase in humidity after the mid-Holocene for the studied region. According to Agatova et al. (2012), a cooling and a minor glacial advance between 3.7 and 3.3 ka BP may have occurred but we did not find any traces in the Mongun-Taiga that would confirm this.

The dated burials of soils (3141–2776 and 1293–1089; Table 2) are in relatively good agreement with the suggested advances at about 2500–3100 (Galakhov et al., 2012) and around about 1700–1800 years ago (Agatova et al., 2012; Galakhov et al., 2012). According to Okishev (2011), ΔZ_0 was 145–190 m for this Historical stage, which slightly exceeds our results (120 m). Okishev (2011) calculated a ΔT of − 1 °C and Galakhov et al. (2005) a ΔT of − 0.4 °C. When using the value − 0.4 °C in our modelling, we obtain an increased precipitation (119%) which agrees well with the Uvs Nuur transgression at that period (Dorofeyuk and Tarasov, 1998; Grunert et al., 2000).

The last glacier advance in the Altai, the LIA or Aktry stage, occurred between the 13th and the 19th century. The maximum LIA glacial advance in the Altai seems to have happened between the 17th and mid-19th century (Ivanovskiy and Panychev, 1978; Ivanovskiy et al., 1982; Ovchinnikov et al., 2002; Okishev, 2011; Nazarov et al., 2016). According to tree-ring measurements and related climatic reconstructions (Myglan et al., 2012) the lowest summer temperatures in the Mongun-Taiga massif were determined for the period 1788–1819. Based on dendrochronological reconstructions (Ganiushkin et al., 2015), the maximum glacial advance took place at the beginning of the 19th century and the glaciers started to retreat after about 1810–1820 AD. Okishev (2011) gives for the Russian Altai an average ΔZ_0 value of 70 m. Lehmkuhl (2012) obtained for the Turgen and Kharkhiraa massifs (Mongolia) a reconstructed ΔELA of 81 and 76 m, respectively. During the last millennia, the treeline position did not change distinctly (Kharuk et al., 2010) because the oscillation of climate was not that strong and treeline position always lags behind climatic change by at least 50, and possibly up to more than 100 years (Körner, 2012).

The reconstructed ΔT values for the LIA maximum in the Altai are − 2 to − 2.5 °C (Adamenko, 1985), − 0.4 °C (Okishev, 2011) and − 0.8 to − 0.9 °C (Okishev, 1985). Summer temperature (June, July) did not seem to have fluctuated that much but winter and mean annual temperatures strongly increased since the LIA in the Altai (Schwikowski et al., 2009). According to Ganiushkin et al., 2015, the climate of the Mongun-Taiga massif was relatively cold and dry during the LIA maximum ($\Delta T = -1.3$ °C, $P = 73\%$). This value correlates well with data from Barnaul, the longest-running meteorological station in the Altai region.

6. Conclusions

Using published and our new data, a chronology of glaciation and the reconstruction of climatic fluctuations in the Mongun Taiga (Altai) was rendered possible for the about the last about 80 ka. We determined high amplitudes of climatic, glacial and treeline changes. The variability (compared to the present-day climate) of summer temperatures ranged from − 3.8 (− 4.2) to + 3.0 °C, precipitation from 43 (37) to 200%, the ELA from − 1200 to 460 m and the upper treeline from − 550 to 470 m. The amount of precipitation was the main factor that determined the timing of the maximal glacial advance in Late Pleistocene. It seems that the MIS 3c and MIS 3a stages were extraordinarily warm. The distinctly elevated treeline during that time evidences that the glaciers retreated to probably high altitudes and covered only a small area. The maximum glacier extent was probably during MIS 4. There is no evidence of a complete disappearance of the glaciers even in the warmest periods of the Late Pleistocene. The precise dating of the LGM, however, still remains open and additional ^{10}Be dates (on suitable boulders) are needed. During several periods, forest vegetation occupied larger areas than today. The actual tendency of warming and increase in precipitation after the LIA maximum probably will lead to a wider expansion of forests.

Acknowledgements

This work was supported by the Saint-Petersburg state University [grant number 18.38.418.2015], the Russian Foundation for Basic Research [grant number 15-05-06611], the All-Russian Public Organization 'Russian Geographical Society' within the framework of the scientific project No. 08/2016-I , by a grant of the Scientific & Technological Cooperation Programme Switzerland-Russia (University of Geneva, nr. 37061135) and Gerald Raab was supported by the Swiss National Science Foundation (SNSF), project grant no. 200021_162338/1. We are, furthermore, indebted to two unknown reviewers for their helpful comments on an earlier version of the manuscript.

References

Adamenko, M.F., 1985. Reconstruction of Summer Temperature Variability and Glacier Dynamics in the Gorniy Altai for Period 14th–20th Centuries. Ph.D. thesis. Press of SBRAS Institute of Geology and Geophysics, Novosibirsk,USSR (in Russian).
Agatova, A.R., Nepop, R.K., Khazina, I.V., Khazin, L.B., 2009. The possibility of the tie correlation of Gorny Altai glaciations to SPECMAP time scale and south Siberia glaciations. In: VI All-Russian Meeting on the Study of the Quaternary Period, pp. 18–20.
Agatova, A.R., Nazarov, A.N., Nepop, R.K., Rodnight, H., 2012. Holocene glacier fluctuations and climate changes in the southeastern part of the Russian Altai (South Siberia) based on a radiocarbon chronology. Quat. Sci. Rev. 43, 74–93. https://doi.org/10.1016/j.quascirev.2012.04.012.
Agatova, A.R., Nepop, R.K., Slyusarenko, I.Yu, Myglan, V.S., Nazarow, A.N., Barinov, V.V., 2014. Glacier dynamics, palaeohydrological changes and seismicity in southeastern Altai (Russia) and their influence on human occupation during the last 3000 years. Quat. Int. 324, 6–19.
Agatova, A.R., Nepop, R.K., 2017. Pleistocene glaciations of the SE Altai, Russia, based on geomorphological data and absolute dating of glacial deposits in Chagan reference section. Geochronometria 44, 49–65. https://doi.org/10.1515/geochr-2015-0059.
Arslanov, K.H.A., Tertychnaya, T.V., Chernov, S.B., 1993. Problems and methods of dating low-activity samples by liquid scintillation counting. Radiocarbon 35, 393–398.
Balco, G., Stone, J.O., Lifton, N.A., Dunai, T.J., 2008. A complete and easily accessible means of calculating surface exposure ages or erosion rates from 10Be and 26Al measurements. Quat. Geochronol. 3, 174–195. https://doi.org/10.1016/j.quageo.2007.12.001.
Blyakharchuk, T.A., 2008. Reconstructing the vegetation of forest and alpine-steppe landscapes in the southwestern part of Tuva since the late glacial period till the present. Geogr. Nat. Resour. 29, 57–62.
Böhlert, R., Egli, M., Maisch, M., Brandová, D., Ivy-Ochs, S., Kubik, P.W., Haeberli, W., 2011. Application of a combination of dating techniques to reconstruct the lateglacial and early Holocene landscape history of the Albula region (eastern Switzerland). Geomorphology 127, 1–13.
Borchers, B., Marrero, S., Balco, G., Caffee, M., Goehring, B., Lifton, N., Nishiizumi, K., Phillips, F., Schaefer, J., Stone, J., 2016. Geological calibration of spallation production rates in the CRONUS-Earth. Quat. Geochronol. 31, 188–198.
Borisov, B.A., Minina, E.A., 1989. Plejstocenovye oledenenija Altae-Sajanskoj gornoj strany i ih korreljacija i rekonstrukcii. In: Paleoklimaty I Oledenenija v Plejstocene. Nauka, Moscow, pp. 217–223.
Borzenkova, I.I., 1984. The climate optimum of the Holocene as a model of the beginning of the 21st century. Meteorol. i Gidrol 8, 69–77 (in Russian).
Borzenkova, I.I., 1992. Izmenenie klimata v kajnozoe. Hydrometeoizdat, Saint-Petersburg.
Bronk Ramsey, C., 2001. Development of the radiocarbon calibration program. Radiocarbon 43, 355–363.
Bronk Ramsey, C., 2009. Bayesian analysis of radiocarbon dates. Radiocarbon 51, 337–360.
Brown, E.T., Edmond, J.M., Raisbeck, G.M., Yiou, F., Desgarceaux, S., 1992. Effective attenuation length of cosmic rays producing ^{10}Be and ^{26}Al in quartz: implications for surface exposure dating. Geophys. Res. Lett. 9, 369–372.
Butvilovskiy, V.V., 1993. Paleogeografiya poslednego oledenenija i holozena Altaja: sobytiyno-katastroficheskaja model'. T.U., Tomsk.
Chistyakov, K.V., Ganyushkin, D.A., Moskalenko, I.G., Zelepukina, E.S., Amosov, M.I., Volkov, I.V., Glebova, A.B., Guzjel, N.I., Zhuravlev, S.A., Prudnikova, T.N., Prjahina, G.V., 2012. Gornyj massiv Mongun-Tajga. V.V.M., Saint-Petersburg.
Christl, M., Vockenhuber, P.W., Kubik, P.W., Wacker, L., Lachner, J., Alfimov, V., Synal, H.-A., 2013. The ETH Zurich AMS facilities: performance parameters and reference materials. Nucl. Instrum. Meth. Phys. Res. B 294, 29–38.
Clark, P.U., Clark, P.U., Dyke, A.S., Shakun, J.D., Carlson, A.E., Clark, J., Wohlfarth, B., Mitrovica, J.X., Hostetler, S.W., Mccabe, A.M., 2009. The last glacial maximum. Science 325, 710–714. https://doi.org/10.1126/science.1172873.
Devyatkin, E., 1965. Cenozoic deposits and neotectonics of southeastern Altai. Proc. GIN AN SSSR 126, 244.
Devyatkin, E.V., 1981. The Cenozoic of Inner Asia (In Russian) (Publ. H. Nauka, Moscow).
Dirksen, V.G., van Geel, B., 2004. Mid to late Holocene climate change and its influence on cultural development in South Central Siberia. In: Scott, E.M., Alekseev, A.Y., Zaitseva, G. (Eds.), Impact of the Environment on Human Migration in Eurasia. NATO Science Series, IV. Earth and Environmental Sciences 42, pp. 159–183.
Dorofeyuk, N.I., Tarasov, P.E., 1998. Vegetation and lake levels in Northern Mongolia in the last 12,500 years as indicated by data of pollen and diatom analysis. Stratigr. Geol. Correl. 70–83.
Galakhov, V.P., Nazarov, A.N., Kharlamova, N.F., 2005. Kolebanija lednikov i izmenenija klimata v pozdnem golocene po materialam issledovanij lednikov i lednikovyh otlozhenij bassejna Aktru (Central'nyj Altaj, Severo-Chujskij hrebet). izdatel'stvo Altajskogo universiteta, Barnaul.
Galakhov, V.P., Chernykh, D.V., Zolotov, D.V., Orlova, L.A., 2012. Polozhenie i vremja formirovanija moren stadij fernau i istoricheskoj v bassejne reki Hajdun na Altae. Izv. Rus. Geogr. Obshchestva 144, 15–21.
Ganiushkin, D., Chistyakov, K., Kunaeva, E., 2015. Fluctuation of glaciers in the southeast Russian Altai and northwest Mongolia mountains since the Little ice age maximum. Environ. Earth Sci. 74, 1883–1904. https://doi.org/10.1007/s12665-015-4301-2.
Ganyushkin, D.A., 2015. Gljaciogennye kompleksy rezkokontinental'nogo rajona severo-zapada Vnutrennej Azii. Glacigenic complexes of sharply continental area of North-west Inner Asia. Saint-Petersburg state university, Saint-Petersburg.
Glazyrin, G.E., 1985. Raspredelenie i rezhim gornyh lednikov. Hydrometeoizdat, Leningrad.
Gosse, J.C., Phillips, F.M., 2001. Terrestrial in situ produced cosmogenic nuclides: theory and application. Quat. Sci. Rev. 20, 1475–1560.
Goudie, A.S., 2006. The Schmidt Hammer in geomorphologlical research. Prog. Phys. Geogr. 30, 703–718. https://doi.org/10.1177/0309133306071954.
Gribenski, N., Jansson, K.N., Lukas, S., Stroeven, A.P., Harbor, J.M., Blomdin, R., Ivanov, M.N., Heyman, J., Petrakov, D.A., Rudoy, A., Clifton, T., Lifton, N.A., Caffee, M.W., 2016. Complex patterns of glacier advances during the late glacial in the Chagan Uzun valley, Russian Altai. Quat. Sci. Rev. 149, 288–305. https://doi.org/10.1016/j.quascirev.2016.07.032.
Grunert, J., Lehmkuhl, F., Walther, M., 2000. Paleoclimatic evolution of the Uvs Nuur basin and adjacent areas (Western Mongolia). Quat. Int. 65–66, 171–192. https://doi.org/10.1016/S1040-6182(99)00043-9.
Herget, J., Carling, P., Agatova, A., Batbaatar, J., Borodavko, P., Gillespie, A., Nepop, R., 2017. Comment on Gribenski, N. et al., 2016. Complex patterns of glacier advances during the late glacial in the Chagan Uzun Valley, Russian Altai. Quaternary Science Reviews 149, 288–305. Quat. Sci. Rev. 168, 216–219. https://doi.org/10.1016/j.quascirev.2017.04.014.
Herren, P.A., Eichler, A., Machguth, H., Papina, T., Tobler, L., Zapf, A., Schwikowski, M., 2013. The onset of Neoglaciation 6000 years ago in western Mongolia revealed by an ice core from the Tsambagarav mountain range. Quat. Sci. Rev. 69, 59–68. https://doi.org/10.1016/j.quascirev.2013.02.025.
IACS, 2011. Glossary of glacier mass balance and related terms. Int. Hydrol. Program. Unit. Nations Educ. Sci. Cult. Organ 86, 114.
Ivanovskiy, L.N., Panychev, V.A., 1978. Razvitie i vozrast konechnyh moren XVII–XIX vv. lednikov Ak-Turu na Altae. In: Processy Sovremennogo Rel'efoobrazovanija v Sibiri. Nauka, Irkutsk, pp. 127–138.
Ivanovskiy, L.N., Panychev, V.A., Orlova, L.A., 1982. Vozrast konechnyh moren stadij «Aktru» i «Istoricheskoj» lednikov Altaja. In: Pozdnij Plejstocen I Golocen Juga Vostochnoj Sibiri. Nauka, Novosibirsk, pp. 57–64.
Ivy-Ochs, S., Kober, F., 2008. Surface exposure dating with cosmogenic nuclides. Quat. Sci. J. 57, 157–189.
Kharuk, V.I., Im, S.T., Dvinskaya, M.L., Ranson, K.J., 2010. Climate-induced mountain tree-line evolution in southern Siberia. Scand. J. For. Res. 25, 446–454.
Klinge, M., 2001. Glacial-geomorphologic Investigations in the Mongolian Altai: a Contribution to the Late Quaternary Landscape and Climate History of Western Mongolia (Aachener Geographische Arbeiten, Aachen).
Körner, C., 2012. Alpine Treelines. Functional Ecology of the Global High Elevation Tree Limits. Springer, Basel.
Korschinek, G., Bergmaier, A., Faestermann, T., Gerstmann, U.C., Remmert, A., 2010. A new value for the half-life of ^{10}Be by heavy-ion elastic recoil detection and liquid scintillation counting. Nucl. Instrum. Methods Phys. Res. Sect. B Beam Interact. Mater. Atoms 268, 187–191.
Kurowsky, L., 1891. Die Hohe der Schneegrenze mit besonderer Berucksichtigung der Finsteraargorngruppe. Pencks Geogr. Abhandlungen 5, 115–160 (in German).
Kubik, P.W., Christl, M., 2010. ^{10}Be and ^{26}Al measurements at the Zurich 6 MV Tandem AMS facility. Nucl. Instrum. Meth. B 268, 880–883.
Lal, D., 1991. Cosmic ray labeling of erosion surfaces: in situ nuclide production rates and erosion models. Earth Planet Sci. Lett. 104, 424–439.
Lehmkuhl, F., 2012. Holocene glaciers in the Mongolian Altai: an example from the Turgen-Kharkhiraa Mountains. J. Asian Earth Sci. 52, 12–20. https://doi.org/10.1016/j.jseaes.2011.11.027.
Lehmkuhl, F., Liu, S., 1994. An outline of physical geography including Pleistocene glacial landforms of Eastern Tibet (provinces Sichuan and Qinghai). Geojournal 34, 7–30. https://doi.org/10.1007/BF00813966.
Lehmkuhl, F., Zander, A., Frechen, M., 2007. Luminescence chronology of fluvial and aeolian deposits in the Russian Altai (Southern Siberia). Quat. Geochronol. 2, 195–201. https://doi.org/10.1016/j.quageo.2006.04.005.

Lehmkuhl, F., Klinge, M., Rother, H., Hülle, D., 2016. Distribution and timing of Holocene and Late Pleistocene glacier fluctuations in western Mongolia. Ann. Glaciol. 57, 169–178.
Malaeva, E.M., 1995. Ob izmenchivosti klimaticheskogo rezhima Gornogo Altaja v pozdnem plejstocene i paleogljaciologicheskih rekonstrukcijah. Geomorfologija 51–60.
Masarik, J., Frank, M., Schaefer, J.M., Wieler, R., 2001. Correction of in-situ cosmogenic nuclide production rates for geomagnetic field intensity variations during the past 800,000 years. Geochem. Cosmochim. Acta 65, 2995–3003.
Matthews, J.A., Shakesby, R.A., 1984. The status of the 'Little Ice Age' in southern Norway: relative age dating of Neoglacial moraines with Schmidt hammer and lichenometry. Boreas 13, 333–346. https://doi.org/10.1111/j.1502-3885.1984.tb01128.x.
Mihaelis, E.P., 1886. An ice-period in Altai mountains. Nature 35, 149.
Murzaeva, V.E., Konopleva, V.I., Devyatkin, E.V., Serebrjanyj, L.R., 1984. Pljuvial'nye obstanovki pozdnego plejstocena i golocena v aridnoj zone Azii i Afriki. Izv. AN SSSR, Ser. Geogr. 15–25.
Myglan, V.S., Oidupaa, O.C., Vaganov, E.A., 2012. A 2367-year tree-ring chronology for the Altay-Sayan region (Mongun-Taiga mountain massif). Archaeol. Ethnol. Anthropol. Eurasia 40, 76–83.
Nazarov, A.N., Myglan, V.S., Orlova, L.A., Ovchinnikov, I.Y., 2016. Aktivnost' lednika Malyj Aktru (Central'nyj Altaj) i izmenenija granicy lesa v bassejne Aktru za istoricheskij period. Led i sneg 56, 103–118.
Nazarov, A.N., Solomina, O.N., Myglan, V.S., 2012. Dinamika verhnej granicy lesa i lednikov Central'nogo i Vostochnogo Altaja v golocene. Dokl. Akad. Nauk 444, 1–5.
Nishiizumi, K., Imamura, M., Caffee, M.W., Southon, J.R., Finkel, R.C., McAninch, J., 2007. Absolute calibration of ^{10}Be AMS standards. Nucl. Instrum. Meth. B 258, 403–413.
Obruchev, V.A., 1914. Altai Sketches (Sketch First). Notes on the Traces of Ancient Glaciation in the Russian Altai. Altajskie jetjudy (jetjud pervyj). Zametki o sledah drevnego oledenenija v Russkom Altae. Zemlevedenie, pp. 50–97.
Okishev, P.A., 1982. Dynamics of Altai Glaciation in the Late Pleistocene and Holocene. T.U., Tomsk.
Okishev, P.A., 1985. Malyj lednikovyj period na Altae. Mater. gljaciologicheskih Issled 170–174.
Okishev, P.A., 2011. Rel'ef i oledenenie Russkogo Altaja (Izd. Tom. un-ta, Tomsk).
Ovchinnikov, D.V., Panyushkina, I.P., Adamenko, M.F., 2002. Millennial larch tree-ring chronology for Mountain Altai and its use for reconstructing summer temperatures. Geogr. Nat. Resour. 102–108.
Peck, J. a, Khosbayar, P., Fowell, S.J., Pearce, R.B., Ariunbileg, S., Hansen, B.C.S., Soninkhishig, N., 2002. Mid to Late Holocene climate change in north central Mongolia as recorded in the sediments of Lake Telmen. Palaeogeogr. Palaeoclimatol. Palaeoecol. 183, 135–153. https://doi.org/10.1016/S0031-0182(01)00465-5.
Pettitt, P.B., White, M., 2012. The British Palaeolithic: Human Societies at the Edge of the Pleistocene World (Routledge, Abingdon).
Pigati, J.S., Lifton, N.A., 2004. Geomagnetic effects on time-integrated cosmogenic nuclide production with emphasis on in situ ^{14}C and ^{10}Be. Earth Planet Sci. Lett. 226, 193–205.
Reimer, P.J., Bard, E., Bayliss, A., Beck, J.W., Blackwell, P.G., Bronk Ramsey, C., Buck, C.E., Cheng, H., Edwards, R.L., Friedrich, M., Grootes, P.M., Guilderson, T.P., Haflidason, H., Hajdas, I., Hatté, C., Heaton, T.J., Hoffmann, D.L., Hogg, A.G., Hughen, K.A., Kaiser, K.F., Kromer, B., Manning, S.W., Nui, M., Reimer, R.W., Richards, D.A., Scott, E.M., Southon, J.R., Staff, A.R.A., Turney, C., van der Plicht, J., 2013. IntCal13 and Marine13 radiocarbon age calibration curves 0–50,000 years cal BP. Radiocarbon 55, 1869–1887.
Revushkin, A.S., 1974. O nahodke iskopaemoj drevesiny na hrebte Mongun-Tajga (Jugo-Zapadnaja Tuva). Izv. Sib. Otd. AN SSSR serija bil 46–47.
Rother, H., Lehmkuhl, F., Fink, D., Nottebaum, V., 2014. Surface exposure dating reveals MIS-3 glacial maximum in the Khangai Mountains of Mongolia. Quat. Res. 82, 297–308. https://doi.org/10.1016/j.yqres.2014.04.006.
Rudaya, N., Tarasov, P., Dorofeyuk, N., Solovieva, N., Kalugin, I., Andreev, A., Daryin, A., Diekmann, B., Riedel, F., Tserendash, N., Wagner, M., 2009. Holocene environments and climate in the Mongolian Altai reconstructed from the Hoton-Nur pollen and diatom records: a step towards better understanding climate dynamics in Central Asia. Quat. Sci. Rev. 28, 540–554. https://doi.org/10.1016/j.quascirev.2008.10.013.
Ruddiman, W.F., McIntyre, A., 1981. Oceanic mechanisms for amplification of the 23,000-year ice-volume cycle. Science 212, 617–627. https://doi.org/10.1126/science.212.4495.617.
Schmidt, E., 1951. A non-destructive concrete tester. Concrete 59 (8), 34–35.
Schwikowski, M., Eichler, A., Kalugin, I., Ovtchinnikov, D., Papina, T., 2009. Past climate variability in the Altai. PAGES News 17, 44–45.
Sergin, V.J., Sergin, S.J., 1978. Sistemnyj analiz programmy bol'shih kolebanij klimata i oledenenija zemli (Hydrometeoizdat, Leningrad).
Shakesby, R.A., Matthews, J.A., Owen, G., 2006. The Schmidt hammer as a relative-age dating tool and its potential for calibrated-age dating in Holocene glaciated environments. Quat. Sci. Rev. 2846–2867.
Sheinkman, V.S., 2002. Testing the S-S technique of TL dating on the Dead Sea sections, its use in the Altai Mountains and palaeogeographic interpretation of results. Archeol. Ethnogr. 10, 22–37.
Sheinkman, V.S., 2011. Glaciation in the high mountains of Siberia. In: Ehlers, J., Gibbard, P.L., Hughes, P.D. (Eds.), Quaternary Glaciations – Extent and Chronology – a Closer Look. Developments in Quaternary Science, vol. 15, pp. 883–907.
Shi, Y., Huang, M., Yao, T., He, Y., 2008. Glaciers and Related Environments in China. Sience Press, Beijing.
Solomina, O.N., 1999. Gornye ledniki Severnoj Evrazii v Golocene (Nauchnyj mir, Moscow).
Stone, J.O., 2000. Air pressure and cosmogenic isotope production. J. Geophys. Res. 105/B10 (23), 753–759.
Svitoch, A.A., Faustov, S.S., 1978. Rezul'taty izuchenija novejshih otlozhenij nekotoryh razrezov Chujskoj vpadiny v svjazi s istoriej oledenenija Gornogo Altaja. In: Sovremennoe I Drevnee Oledenenie Ravninnyh I Gornyh Rajonov SSSR (Sbornik Statej). Izd-vo GO SSSR, pp. 114–124.
Thompson, L.G., 1997. Tropical climate instability: the last glacial cycle from a Qinghai-Tibetan ice core. Science 276 (80), 1821–1825. https://doi.org/10.1126/science.276.5320.1821.
Van Meerbeeck, C.J., Renssen, H., Roche, D.M., 2008. How did Marine isotope stage 3 and last glacial maximum climates differ? Perspectives from equilibrium simulations. Clim. Past Discuss 4, 1115–1158. https://doi.org/10.5194/cpd-4-1115-2008.
Velichko, A.A., Klimanov, V.A., Borzenkova, I., 2009. Klimaticheskie harakteristiki golocena (6000-5500 l.n.) (karty 6–10). In: Paleoklimaty I Paleolandshafty Vnetropicheskogo Prostranstva Severnogo Polusharija. Pozdnij Plejstocen – Golocen. Atlas-monografija. Geos, Moscow, pp. 20–24.
Voelker, A.H.L., Workshop participants, 2002. Global distribution of centennial scale records for Marine isotope stage (MIS) 3: a database. Quat. Sci. Rev. 21, 1185–1212.
von Blanckenburg, F., Belshaw, N.S., O'Nions, R.K., 1996. Separation of ^{9}Be and cosmogenic ^{10}Be from environmental materials and SIMS isotope dilution analysis. Chem. Geol. 129, 93–99.
Xu, X., Yang, J., Dong, G., Wang, L., Miller, L., 2009. OSL dating of glacier extent during the last glacial and the Kanas lake basin formation in Kanas river valley, Altai mountains, China. Geomorphology 112, 306–317. https://doi.org/10.1016/j.geomorph.2009.06.016.
Zhao, J., Yin, X., Harbor, J.M., Lai, Z., Liu, S., Li, Z., 2013. Quaternary glacial chronology of the Kanas river valley, Altai mountains, China. Quat. Int. 311, 44–53. https://doi.org/10.1016/j.quaint.2013.07.047.